AIR-DEHUMIDIFICATION BY MEANS OF ABSORBED COLUMN

Joselma Araújo de Amorim, joselmaaraujo@yahoo.com.br
PPGEM/CT/UFPB, João Pessoa, Paraíba, Brazil

Márcia Ramos Luiz, marciaramosluiz@yahoo.com.br
PPGEM/CT/UFPB, João Pessoa, Paraíba, Brazil

José Maurício Gurgel, jmgurgel@pq.cnpq.br
LES/DEM/UFPB, João Pessoa, Paraíba, Brasil

Abstract. *The present work is about the mathematical modeling and the numeric simulation of heat transfer along an adsorbed column used for the dehumidification of humid air. A computational code was developed to simulate the influence of some of the physical aspects, and a computational code was developed to simulate the influence of some of the physical and geometric parameters on the dynamic sorption of both the charge (adsorption) and the discharge (regeneration) of the adsorptive reactors for dehumidification. The differential equations were solved be means of the method of finite volumes. The solution for the linear systems made up by the discretized equations was obtained via Thomas' algorithm (TDMA). Various numeric results are offered for the loading of a cylindrical column measuring 0.5m in length filled up with 5mm dyameter grains silica gel. In the adsorptive process, the silica gel bed was submitted to three conditions of relative humidity (50, 70 and 100%) as given at both the entrance of the column and during the regeneration, three temperatures of regeneration had been used (70, 90 and 100 ºC) . The results have been given as temperature profiles and adsorbed mass at the outlet of the column according to time. These results were shown to be physically consistent with the desired outlet condition.*

Keywords: *Method of Finite Volumes, Modeling, Dehumidification and TDMA.*

1. INTRODUCTION

The process of air dehumidification by means of compacted beds is used for several industrial purposes, among which we can highlight the following: in the food industry and that of pharmaceuticals in order to avoid absorption of humidity in hygroscopic products; in place of air-conditioned conventional systems, for it does not use cooling gas, preserving, in this way, the ozone layer. One of the advantages of the utilization of compacted beds in air dehumidification stems from the low operational cost, and, the pollution free capabilities this process involves, for it does not use poisonous gases and it can be fully regenerated under low temperatures with the use of solar energy.

Silica gel, alumina and activated coal are the adsorptive material most employed in compacted beds; however, a number of studies have demonstrated that silica gel is the micro porous solid most used in processes of air dehumidification. This is due to its specific surface, which is quite elevated, and may reach 800 m^2/g, propitiating a highly desiccant capability to the point of adsorbing water at a rate of 40% of its weight – a quantity superior to that adsorbed by alumina (RUTHVEN, 1984).

In view of all these factors, a number of authors have developed studies on air dehumidification processes in compacted beds, some of which will be mentioned here: Park and Knaebel (1992) studied water vapor adsorption on silica gel fixed bed by assessing the humidity content found in humid air as it passes through the bed. Hamed (2002) carried out an experimental numeric study to determine the transient form and the adsorption characteristics in vertical beds. Inaba and Horibe (2004) investigated from a numeric viewpoint the adsorption in a rectangular bed filled up with silica gel when exposed to humid airflow. Awad et al (2008) studied both experimentally and numerically the dehumidification of compacted beds when exposed to a radial airflow. The regeneration of compacted beds connected to solar collectors was examined by Saito (1993), Techajunta et al (1999) and Surajitr (2007). San and Jiang (1994) had also tested and modeled regeneration in compacted beds by taking into account the best performing time under three different regenerating temperatures: 65, 75 and 85°C. Singh and Singh (1998) studied sílica gel regeneration in multi-shelf regenerators at temperatures varying from 42 to 72°C, and varying speed from 0.175 to 0.55 m/s. The effects of temperature and the time of regeneration during the dehumidification processes using modified, commercial silica gel were studied by Chang et al (2004). Kabeel (2009) carried out an experimental numeric study in compacted beds to evaluate their performance in both adsorptive and desorptive processes.

The purpose of this work is to carry out a numerical investigation on the effects caused by different level of humidity during desorption processes implementing the optimization of adsorptive reactors for air dehumidification.

2. MATHEMATICAL MODELING

Figure 1 shows the adsorption dynamic on a compacted bed. During the adsorptive process, the bed compacted with adsorptive material (silica gel) was submitted to a humid airflow under prescribed conditions at the column inlet, and in the adsorptive process different dehumidified hot airflows were used at the bed inlet.

Mass and heat transfer equations have been used for the present study, based on simplifying hypotheses that resulted in mass diffusion on non-isotherm grains and in adsorptive compacted bed.
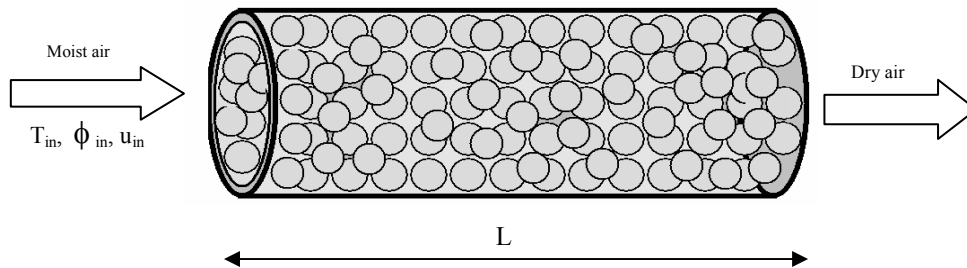
Figure 1 – Compacted bed diagram.

Due to the complexity of the equations, some simplifying hypotheses have been taken into account to facilitate the mathematical modeling. These were:

- The airflow exhibits constant velocity along the column;
- Radial effects have been neglected;
- Charge losses along the column have been neglected;
- Transportation within the compacted bed occurs by means of convection and heat diffusion;
- The adsorbate behaves like an ideal gas;
- Both the temperature and the effective mass coefficient on the adsorbent grain have considered uniform;
- The instantaneous balance on the grain surface has been taken into account.

Figure 2 illustrates simplification on a numerical approach in circumstances when the adsorptive bed is made up of various control volumes where each volume is represented by a single, homogeneous, spherical and adsorbent grain that has been submitted to humid airflow on the charge (adsorption) and to hot airflow on the discharge (regeneration). Without this simplification, the exact representation of the compacted bed would be rendered excessively complex, requiring too much computational time in order to obtain the necessary solutions.
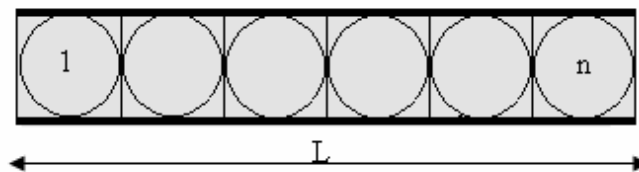
Figure 2 – Compacted bed diagram for an adsorbent grain for each control volume.

After considering the simplifying hypotheses, the mass and energy diffusion models will be presented for the grains along with the model for the adsorptive compacted bed in subsections 2.2 and 2.3, respectively.

2.2 Grain Model

The mathematical model proposed for the grains is represented by the continuity equation and by the energy conservation equation, respectively.

$$\frac{\partial q}{\partial t} = \frac{1}{r^2}\frac{\partial}{\partial r}\left(r^2 D_{ef}\frac{\partial q}{\partial r}\right) \tag{1}$$

$$C_S \frac{\partial T_S}{\partial t} = \frac{6 h_P}{d_P} (T_f - T_S) + (-\Delta H) \frac{\partial \overline{q}}{\partial t} \tag{2}$$

The Equation (3) determines the average water quantity present in the grain.

$$\overline{q} = \frac{3}{R_p} \int_0^{R_p} q(r,t) r^2 dr \tag{3}$$

The initial and contour conditions for equations (1) and (2) are:

$$t < 0: \qquad q(r,t) = q^*(p_0, T_0) \quad ; \quad T_S(t) = T_0 \qquad \text{for} \qquad 0 \le r \le R_p \tag{4}$$

$$r = 0: \qquad \frac{\partial q(r,t)}{\partial t} = 0 \qquad \text{for} \qquad t > 0 \tag{5}$$

$$r = R_p: \qquad q(r,t) = q^*(p, T_S) \qquad \text{for} \qquad t > 0 \tag{6}$$

2.3 Adsorptive compacted bed model

Mass transfer equation for the mixture:

$$\frac{\partial \rho_m}{\partial t} + \frac{\partial}{\partial x}(u \rho_m) = -\frac{1-\varepsilon}{\varepsilon} \frac{\partial \overline{q}}{\partial t} \tag{7}$$

Mass transfer equation for water vapor:

$$\frac{\partial \rho_v}{\partial t} + \frac{\partial}{\partial x}(u \rho_v) = \frac{\partial}{\partial x}\left(D_L \frac{\partial \rho_v}{\partial x}\right) - \frac{1-\varepsilon}{\varepsilon} \frac{\partial \overline{q}}{\partial t} \tag{8}$$

The axial dispersion coefficient of humid airflow on the compacted bed adsorption may be represented by the following equation (Ruthven, 1984):

$$D_L = \gamma_1 D_m + \gamma_2 \, 2 \, R_p \, u \tag{9}$$

Balance energy equation for the column adsorption:

$$\frac{\partial}{\partial t}(C_M T_f) + \frac{\partial}{\partial x}(C_M u T_f) = \frac{\partial}{\partial x}\left(\frac{\lambda_f}{cp_f} \frac{\partial T_f}{\partial x}\right) + \frac{6 h_p}{d_p} \frac{(1-\varepsilon)}{\varepsilon cp_f}(T_s - T_f) + \frac{2U_g(T_\infty - T_f)}{\varepsilon R_i cp_f} \tag{10}$$

Where

$$p_v = \rho_v R_g T_f \tag{11}$$

$$C_M = \rho_m cp_m \tag{12}$$

The initial contour conditions are:

$$t < 0: \quad \rho_v(x,t) = \rho_0; \quad \rho_m(x,t) = \rho_0; \quad T_f(x,t) = T_0 \qquad \text{for} \quad 0 \le x \le L \tag{13}$$

$$x = 0: \quad \rho_v(x,t) = \rho_{vin}; \quad \rho_m(x,t) = \rho_{min}; \quad T_f(x,t) = T_{in} \qquad \text{for} \quad t \ge 0 \tag{14}$$

$$x = L: \quad \frac{\partial \rho_v(x,t)}{\partial t} = 0; \quad \frac{\partial \rho_m(x,t)}{\partial t} = 0; \quad \frac{\partial T_f(x,t)}{\partial t} = 0 \qquad \text{for} \quad t \ge 0 \tag{15}$$

2.3.1 Determining the heat transfer coefficient on the wall:

Equation (16) represents the heat transfer coefficient on the wall, as determined by the sum of the intern and extern resistances, and on the column wall (Ruthven, 1984).

$$U_g = \cfrac{1}{\cfrac{1}{h_i} + \cfrac{R_i}{\lambda_w}\ln\left(\cfrac{R_e}{R_i}\right) + \cfrac{R_i}{R_e}\cfrac{1}{h_e}} \tag{16}$$

According to Ruthven, the internal convection coefficient may be determined by the following equation:

$$Nu_i = \frac{h_i D_i}{\lambda_f} = 0.813\,Re^{0.19}\,e^{-6dp/Di} \tag{17}$$

The external convection coefficient was determined by Equation (18), and forced convection conditions were adopted (Incropera e DeWitt, 2002).

$$Nu_e = \frac{h_e D_e}{\lambda_{air}} = 0.193\,Re^{0.618}\,Pr^{1/3} \tag{18}$$

3. NUMERICAL TREATMENT

Equations (1), (7), (8) and (10) were discretized by means of finite volume methods (Maliska, 1995). The Upwind interpolation system was employed in order to evaluate the properties of the control volumes interface. Equations (1), (7), (8) and (10) were integrated to both space and time generating the following equation:

$$A_p\varphi_P = A_e\varphi_E + A_w\varphi_W + B \tag{19}$$

Where φ may be q, ρ_v, ρ_m e T_f, depending on the desired equation. Each equation that has been obtained is one-dimensional, forming in this way a tri-diagonal matrix. .

The system's solution procedure will be interactive, solving one equation at a time. In order to solve the system of linear equations provided by Equation (19), Thomas' algorithm (TDMA) was used (Maliska, 1995).

The convergence criterion used to interrupt the interactive process was the following:

$$\left|\frac{\phi_P^{k+1} - \phi_P^k}{\phi_{max} - \phi_{min}}\right| \leq 10^{-5} \tag{20}$$

Where $\left|\phi_{max} - \phi_{min}\right|$ represents the maximum and minimum variations of the fluid phase obtained after a n-iterations. Another iteration will be required as long as such condition is not verified.

4. RESULT DISCUSSION

4.1 Model Validation

The model was validated by using the experimental data provided by Park and Knaebel (1992). The validation demonstrated that the model represented very well the phenomenon, exhibiting strong coherence with the experimental data graphically presented by Amorim (2007).

4.2 Numeric Results

Table 2 shows the properties of both the adsorbate (humid air) and the adsorbent (Silica gel Sorbead, type C) that have been used in the numeric simulation. Some of the properties shown in this table came from Santos (2005). Some other properties useful to the simulation were obtained through the equations found in Amorim (2007). On the other hand, the global and dispersion coefficients on the column wall were calculated by means of Equations (9 and 16).

Table 2: Properties of both the adsorbent and the adsorbate used in the simulation.

Parameters	Symbols	Values
Grain radius	R_g	$2,5 \times 10^{-3}$ m
Column Length	L	0,5 m
Column inner radius	R_i	0,02 m
Initial column temperature	T_o	308 K
Air relative humidity	ϕ_∞	70, 90 e 100 %
Interstitial velocity	u	0,5; 1; 2 e 3 m/s
Axial dispersion coefficient	D_L	Eq. (9)
Adsorption heat	ΔH	3×10^6 J/kg
Bed porosity	ε	0,4
Adsorbent density	ρs	1270 kg/m3
Inlet air temperature	T	323, 363 e 373 K
Heat transfer coefficient on the wall [W/m2 K]	U_g	Eq. (16)
Adsorbent specific heat	Cp_s	1074 J/kg K

4.2.1 Relative humidity influence on the compacted bed inlet.

The influence of relative humidity over the charging process on compacted bed can be seen through the mass adsorbed profile and through the temperature at the column outlet. For the present study, three aspects of relative humidity at the column outlet (50, 70 and 100%) have been considered. These conditions were simulated by considering one column with a length equal to 0.5 m and a velocity of 0.5 m/s.

Figure 3 show that with an increase in relative humidity an increase in pressure is also verified to occur on the vapor molecules present in the air. This increase in pressure causes the front mass to advance enabling the airflow to surpass the resistance along the column and achieve the last control volume saturation point much faster. It has been seen as well that, with an increase in humidity, an increase in mass quantity adsorbed by the grains could be seen in the graphic as representing a variation of 0.252 to 0.406 kg of water vapor/kg silica. This is due to the fact that the grain balance concentration is directly related to an increase in the water vapor present in the air, and also to the maximum capacity of grain adsorption.
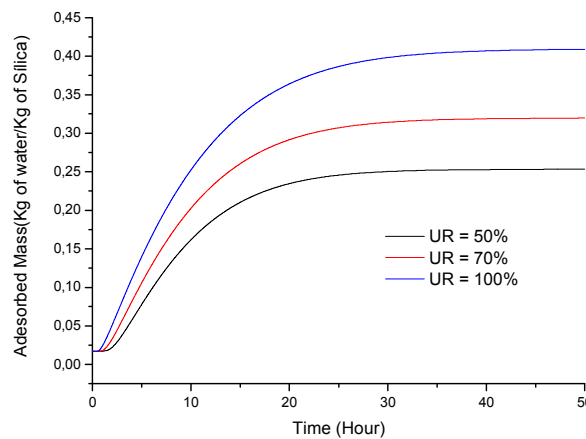
Figure 3: Relative humidity influence over the adsorbed mass at the compacted bed outlet.

Figure 4 shows temperature increase as a result of an increase in humidity. However, this had already been anticipated, for with the increase of the adsorption rate there occurred an increase in fluid temperature due to the heat produced by the grains during adsorption. Temperature may get as high as 45, 49, 55°C, when humidity equals 50, 70 and 100%.
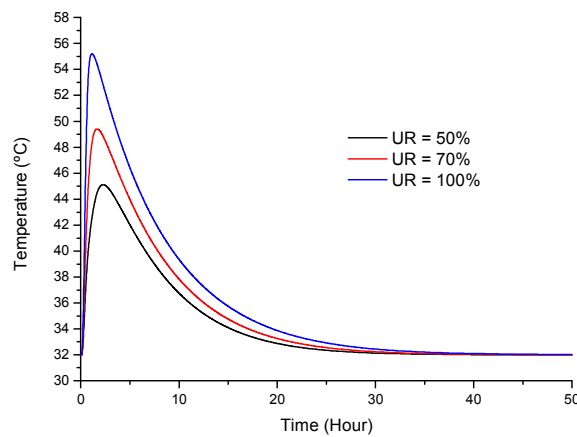
Figure 4: Relative humidity influence over the air temperature profile at the compacted bed outlet.

4.2.2 Regeneration temperature influence over the compacted bed desorption process

Figure 5 describes the incoming air temperature effect in the regeneration of compacted bed at temperature levels of 70, 90 and 100% at some uniform out-flowing air velocity of 3m/s. One can verify an increase in the maximum quantity of desorbed mass with a rise in temperature of about 0.0397; 0.0177, 0.0119 kg of silica water/kg for temperatures of 70, 90 and 100%, respectively. This may be seen as the result of a decrease in water vapor pressure in the air, which is directly related to temperature.

(3a)

(3b)
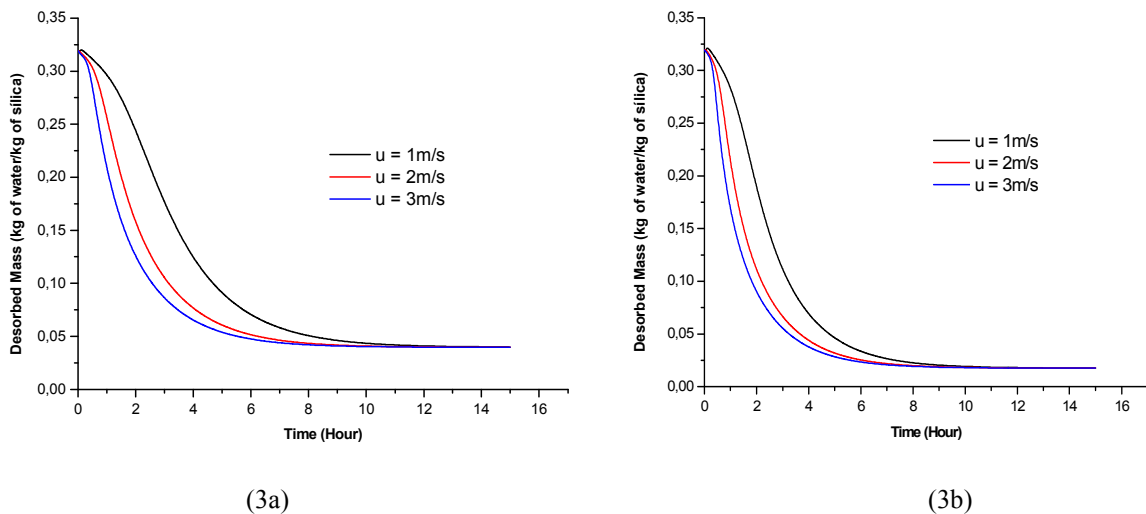
Figure 5: Air velocity influence over the desorptive process at the compacted bed outlet.

4.2.3 Regeneration temperature influence over the compacted bed desorptive process

Figure 6 describes the effect of the in-coming air temperature on compacted bed regeneration for temperature values around 70, 90 and 100% at constant air velocity of 3m/s. One can see an increase in the maximum quantity of desorptive mass with an increase in temperature round 0.0397, 0.0172, 0.0119 kg water/kg of silica for temperatures of 70, 90 and 100°C, respectively. This may occur in connection with the water vapor pressure present in the air that is directly related to temperature.
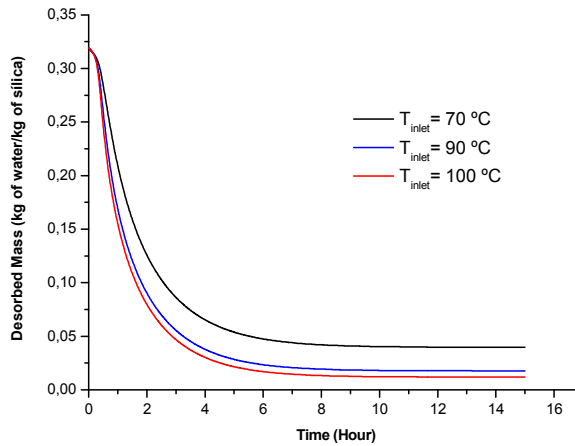
Figure 6: Regeneration temperature influence over the desorptive process at the compacted bed outlet.

4.2.4 The influence of effective mass diffusion coefficient over compacted bed regeneration

Figure 7 shows the influence of effective mass diffusion on the grain close to the compacted bed outlet during the regeneration process. From this figure one can see that the smaller the diffusion coefficient, the slower is the front mass propagation along the compacted bed. This is due to a lesser resistance to mass diffusion in the grains, and as this coefficient increases, the faster the propagation will be, the greater will be the resistance. This produces a greater quantity of water vapor during the desorptive process.
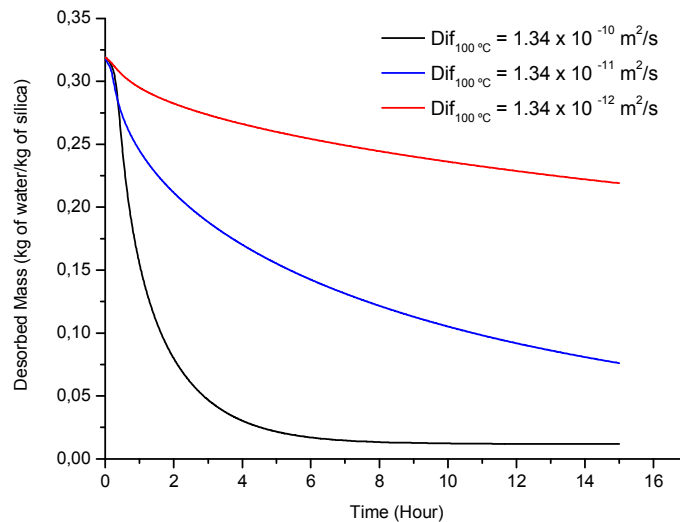
Figure 7: Regeneration temperature influence over the desorptive process at the compacted bed outlet.

5. CONCLUSIONS

In the light of the results obtained by means of numeric simulation of mass and heat transfer equations to examine the proposed mathematical model for both the desorption and adsorption dynamics, one concludes that an increase in humidity during the adsorptive process causes both the quantity of mass absorbed by the grains and bed temperature to increase. During the desorptive process, one could observe that an increase in flow velocity for both temperatures reduced regeneration time to approximately three hours. For different temperatures, it has been concluded that, the higher the temperature of regeneration, the greater will be the quantity of water vapor desorbed by the bed. As for the case of the diffusion coefficient, it has been concluded that the greater this coefficient is, the most recommended it is for the desorptive process. This is because there occurs a faster and larger quantity of water vapor release during the process.

6. REFERENCES

Amorim, J. A., "Caracterização de uma Coluna de Sílica Gel para desumidificação". Dissertação de Mestrado, Engenharia Mecânica, UFPB, 2007.

Hamed, A.M.; Theoretical and experimental study on the transient adsorption characteristics of vertical packed porous bed, Renewable Energy 37 (2002), pp. 525–541.

Incropera, F.P.; DeWitt, D.P. ; "Fundamentals of Heat and Mass Transfer", Wiley & Sons, 4ª Ed., 1996.

Inaba, H., Seo, J.K. and Horibe, A., 2004, "Numerical Study on Adsorption Enhancement of Rectangular Adsorption Bed", Heat Mass Transfer, 41, 133-146.

Kabeel, A. E.; "Adsorption–Desorption Operations of Multilayer Desiccant Packed Bed for Dehumidification Applications". Renewable Energy 34 (2009), pp. 255–265.

Kuei-Sen Chang, Hui-Chun Wang and Tsair-Wang Chung, Effect of regeneration conditions on the adsorption dehumidification process in packed silica gel beds, Applied Thermal Engineering 24 (2004), pp. 735–742.

Maliska, C. R., 1995, "Computational Fluid Mechanics and Heat Transfer", LTC, Rio de Janeiro, Brazil, 135-137, 185-186.

Park, I.; Knaebel, K. S., "Adsorption Breakthrough Behavior: Unusual Effects and Possible Causes", AIChE Journal, v. 38, n. 38, p. 660-670, 1992.

P. Surajitr and R.H.B. Exell, The regeneration of silica gel desiccant by air from a solar heater with a compound parabolic concentrator, Renewable Energy 32 (2007), pp. 173–182.

Ruthven, D.M., 1984, "Principles of Adsorption Processes". Wiley Interscience, New York, 1984.

Santos, J. C., "Análise Numérica da Dinâmica de Adsorção em Coluna Aplicada ao armazenamento de Gás Natural". Tese de Doutorado, Engenharia Mecânica, UFPB, 2005.

San, J. Y. and Jiang, G.D.; 1994, "Modeling and Testing of a Silica Gel Packed – Bed System", Internat. J. Heat Mass Transfer, 37, pp. 1173-1179.

Saito, Y.; Regeneration characteristics of adsorbent in the integrated desiccant/collector, Journal of Solar Energy Engineering 115 (1993), pp. 169–175.

Singh, S. and Singh, P.P.; Regeneration of silica gel in multi-shelf regenerator, Renewable Energy 13 (1) (1998), pp. 105–119.

S. Techajunta, S. Chirarattananon and R.H.B. Exell, Experiments in a solar simulator on solid desiccant regeneration and air dehumidification for air conditioning in a tropical humid climate, Renewable Energy 17 (1999), pp. 549–568.

7. ACKNOWLEDGEMENTS

8. NOTE OF RESPONSIBILITY

The author(s) is (are) the sole responsible for the printed material included in this paper.

NOTATION

Cp Calor específico à pressão constante [J/kg K]
C_S Capacidade volumétrica do sólido [J/m³ K]
C_m Capacidade volumétrica da mistura [J/m³ K]
d_p Diâmetro do grão [m]
D_{ef} Coeficiente de difusão de massa [m²/s]
D_L Dispersão axial [m²/s]
q Concentração do sólido [kg/m³]
$\overline{q}$ Concentração media do grão [kg/m³]
u Velocidade intersticial [m/s]
h Coeficiente de transferência de calor [W/m² K]
ΔH Calor de adsorção [J/kg]
L Comprimento da coluna [m]
Nu Número Nusselt
p Pressão [Pa]

Pr Número de Prandtl
r Coordenada radial do grão [m]
R Raio da coluna [m]
R_e Número de Reynolds
R_g Constante do gás ideal [J/kg K]
t Tempo [s]
T Temperatura [K]
U_g Coeficiente global na parede [W/m² K]

Letras gregas
ε Porosidade do leito
λ Condutividade térmica [W/m K]
ρ Massa especifica [kg/m³]
ϕ Umidade relativa do ar [%]

Superscript
* Relativo ao equilíbrio de adsorção
x Coordenada axial da coluna [m]

Subscritos
∞ Relativo à condição ambiente
0 Relativo à condição inicial
e Relativo à superfície externa
f Relativo à fase fluida
I Relativo à superfície interna
in Relativo a entrada da coluna
p Relativo ao grão
S Relativo à fase sólida
w Relativo à parede da coluna

a Ar seco
v Vapor d'água
m gás (ar seco + vapor d'água)